Supporting Information

High pressure synthesis, crystal chemistry and ionic conductivity of structural polymorph of $Li_3BP_2O_8$

Eiichi Hirose[*,†], Kunimitsu Kataoka[§], Hiroshi Nagata[§], Junji Akimoto[§], Takuya Sasaki[‡], Ken Niwa[‡], Masashi Hasegawa[*,‡]

[†]*Department of Crystalline Materials Science, Graduate School of Engineering, Nagoya University*
Furo-cho, Chikusa-ku, Nagoya
Aichi 464-8603, Japan

[‡] *Department of Materials Physics, Graduate School of Engineering, Nagoya University*
Furo-cho, Chikusa-ku, Nagoya
Aichi 464-8603, Japan

[§]*National Institute of Advanced Industrial Science and Technology (AIST)*
AIST Tsukuba Central 5, 1-1-1 Higashi, Tsukuba
Ibaraki 305-8565, Japan

Corresponding Author:

*E-mail: hirose.eiichi@f.mbox.nagoya-u.ac.jp

*E-mail: hasegawa@mp.pse.nagoya-u.ac.jp

Experimental Section

The mixture powder of Li_3PO_4 and BPO_4 with equimolar ratio was enclosed in a BN capsule. The synthesis was carried out at 2 & 4 GPa and 600 °C using a DIA-type multi-anvil press apparatus. After keeping the sample at high pressure and temperature for 30 minutes, it was cooled to room temperature. Then, the sample was recovered at ambient pressure and it was characterized by the powder X-ray diffraction (XRD, Cu-Kα) measurements (Rigaku Co., RINT-2500VB2). The synchrotron powder XRD experiments were also conducted at the BL5S2 of the Aichi Synchrotron Radiation Center, Aichi Science & Technology Foundation, Aichi, Japan. The wavelength (0.74985 Å) was calibrated prior to the sample measurements. The dedicated software of Jana2006 and VESTA were used for solving and drawing the crystal structure, respectively.[1,2] The polycrystalline HP-$Li_3BP_2O_8$ was shaped into the disk with diameter and thickness of 4.5 mm and 0.5 mm, respectively. The relative density of the polycrystalline HP-$Li_3BP_2O_8$ bulk sample disk was approximately 91 %. The lithium ionic conductivity measurements were performed with AC impedance method using an impedance analyzer (Solartron 1260) in a frequency range of 1 ~ 10^7 Hz at temperatures comprised between 375 K and 456 K in flowing N_2 gas, with an applied voltage of 0.5 V. Au paste was used as the electrode.

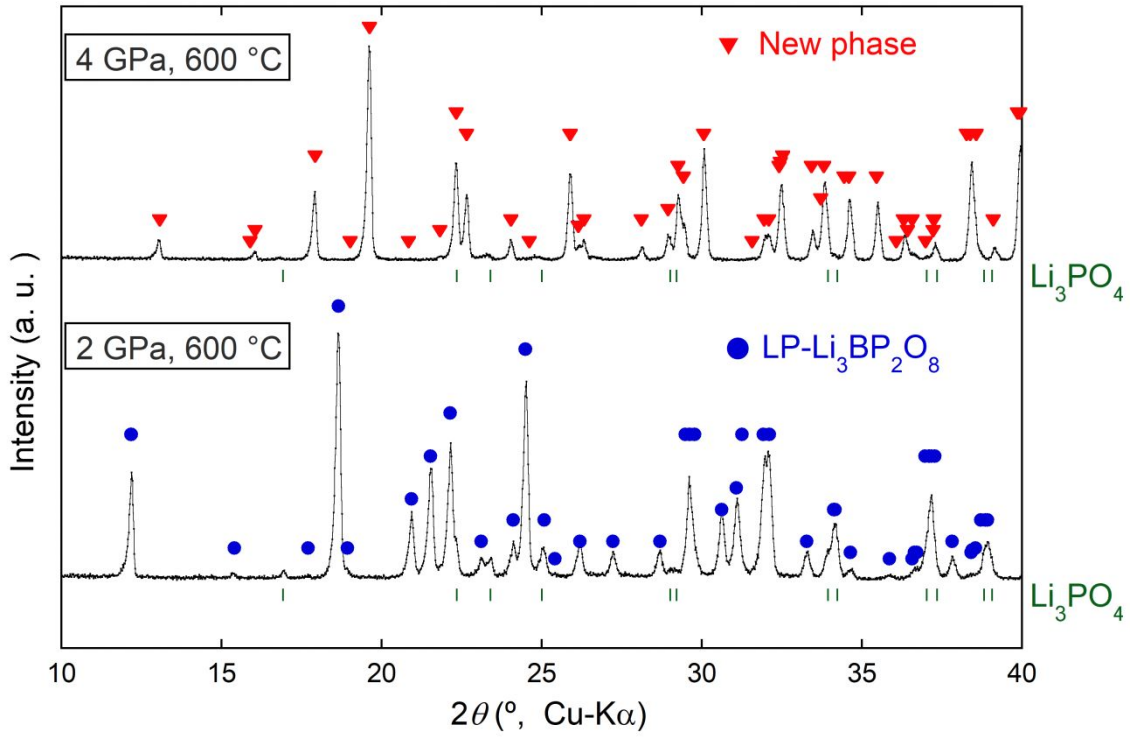

Figure S1. X-ray diffraction profiles of the ambient recovered samples from the synthesis experiments at high pressures (2 GPa - 600 °C and 4 GPa - 600 °C). The blue circles and red triangles correspond to LP-$Li_3BP_2O_8$ and new phase (HP-$Li_3BP_2O_8$), respectively. The green tips represent the Bragg peak positions of Li_3PO_4.

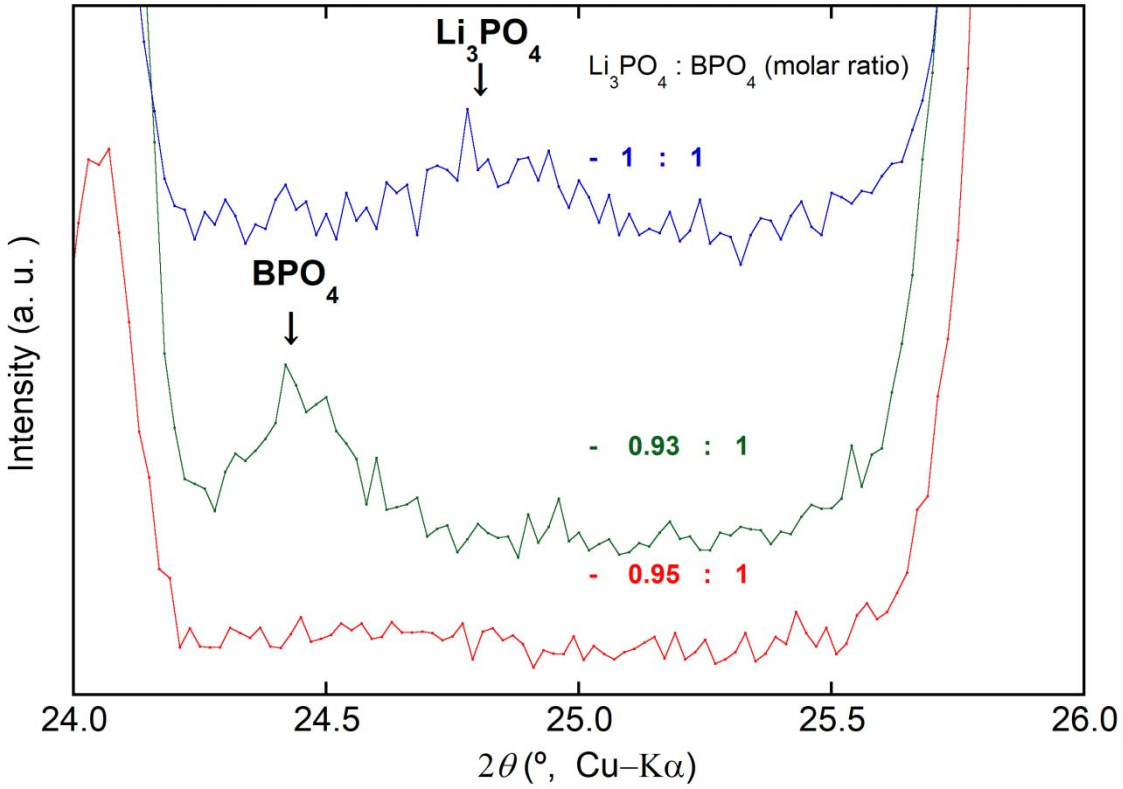

Figure S2. X-ray diffraction profiles of the ambient recovered samples from the synthesis experiments at high pressures (4 GPa - 600 °C) using powder mixtures of Li_3PO_4 and BPO_4, composition ratio of Li_3PO_4 : BPO_4 molar ratio of 1 : 1, 0.93 : 1 and 0.95 : 1.

Table S1. The calculated bond lengths and bond valence sums (V_i) for HP-$Li_3BP_2O_8$.

Li1-O1 [i]	1.902(6)	B1-O2	1.469(4)
Li1-O6 [ii]	2.003(6)	B1-O4 [x]	1.468(5)
Li1-O6 [iii]	2.067(6)	B1-O5	1.492(5)
Li1-O8 [iii]	2.017(6)	B1-O7 [xi]	1.513(4)
V_{Li1}	1.069(8)	V_{B1}	2.992(18)
Li2-O1 [iv]	1.923(7)	P1-O1	1.527(2)
Li2-O3 [v]	2.227(7)	P1-O4	1.578(2)
Li2-O4 [vi]	2.506(6)	P1-O5	1.604(3)
Li2-O5 [v]	2.457(6)	P1-O6	1.494(2)
Li2-O7 [iii]	2.160(7)	V_{P1}	5.055(15)
Li2-O8 [vii]	2.022(7)		
V_{Li2}	0.960(8)	P2-O2	1.567(3)
		P2-O3	1.502(2)
Li3-O1 [viii]	2.150(7)	P2-O7	1.608(2)
Li3-O2 [viii]	2.470(6)	P2-O8	1.534(2)
Li3-O3 [ix]	1.836(6)	V_{P2}	5.046(16)
Li3-O5 [iii]	2.737(7)		
Li3-O6	2.053(6)		
Li3-O8 [viii]	2.166(6)		
V_{Li3}	1.009(8)		

symmetry codes: (i) -x+1/2,y+1/2,-z; (ii) -x+1/2,y+1/2,-z+1; (iii) x-1/2,-y+1/2,z; (iv) -x+3/2,y+1/2,-z; (v) -x+3/2,y+1/2,-z+1; (vi) -x+1,-y+1,-z; (vii) x,y+1,z; (viii) -x+1,-y,-z; (ix) -x+1,-y,-z+1; (x) x+1/2,-y+1/2,z; (xi) -x+2,-y,-z+1.

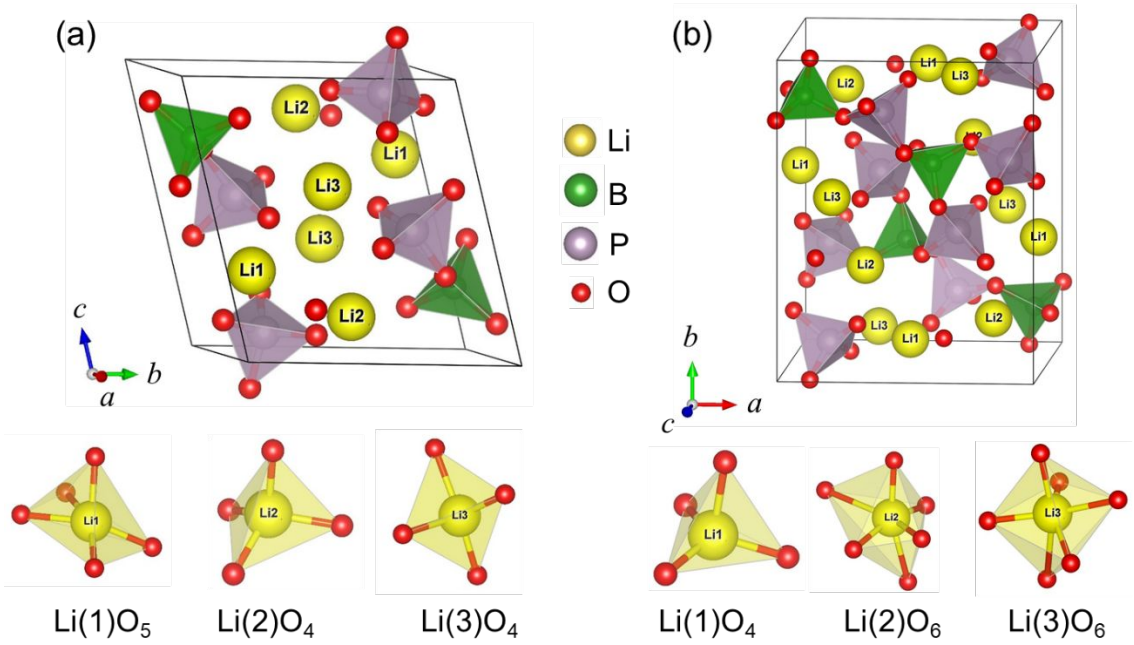

Figure S3. The crystal structures of LP-$Li_3BP_2O_8$[3] and HP-$Li_3BP_2O_8$.

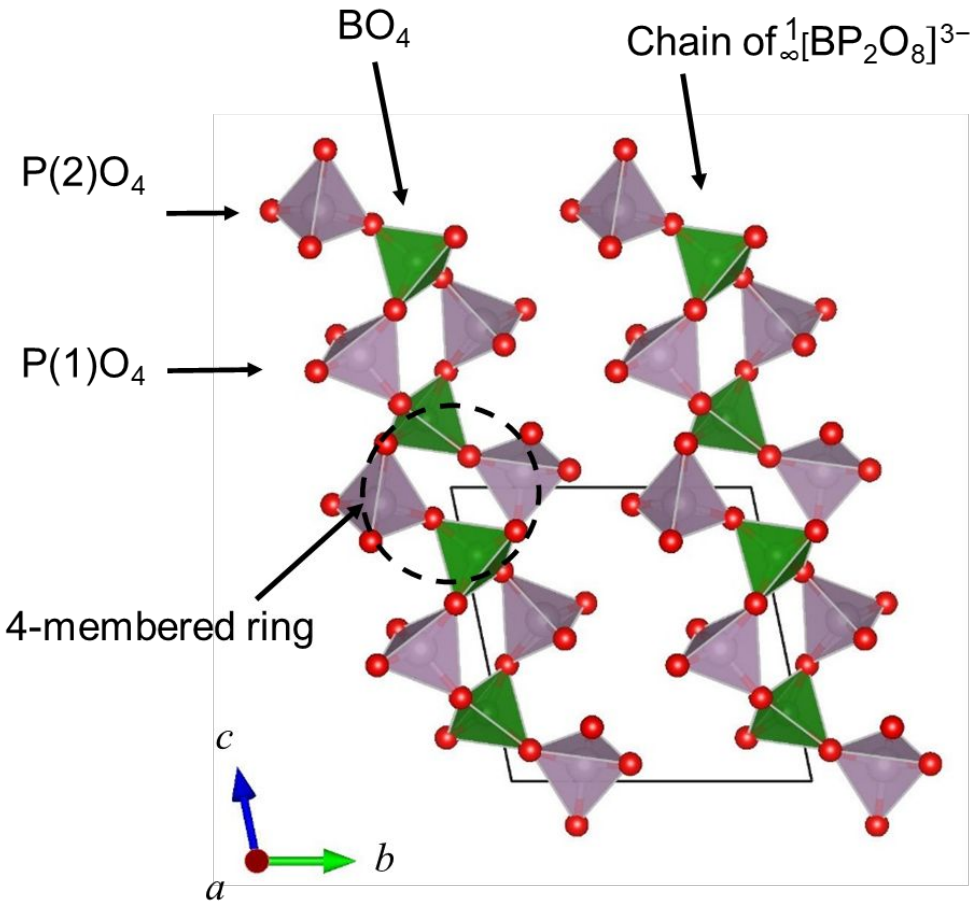

Figure S4. The projective view of the crystal structure of $^{1}_{\infty}[BP_2O_8]^{3-}$ in LP-$Li_3BP_2O_8$.

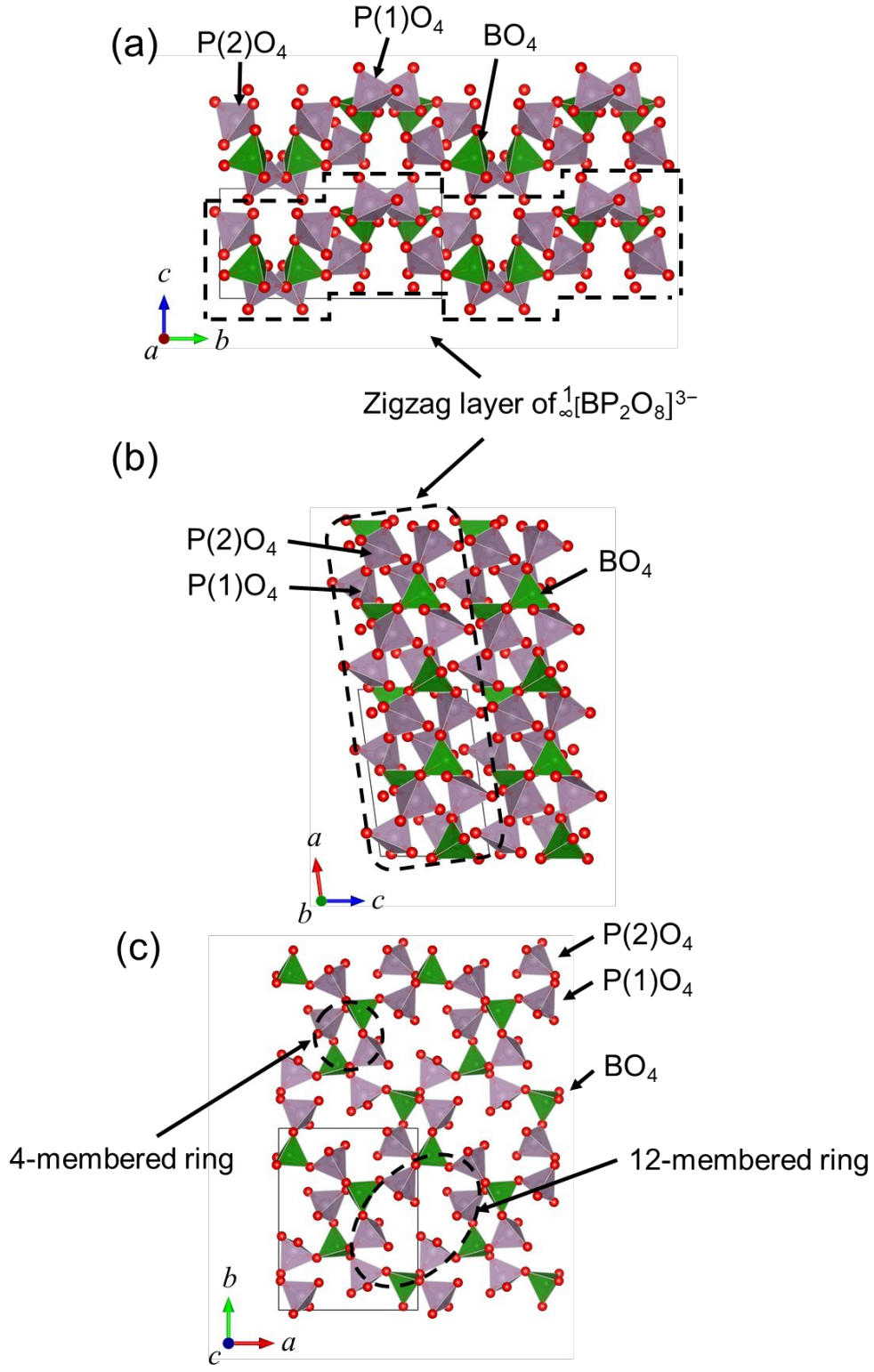

Figure S5. The projective views of the crystal structure of $[BP_2O_8]^{3-}$ in HP-$Li_3BP_2O_8$ along (a) the *a* axis, (b) *b* axis and (c) *c* axis.

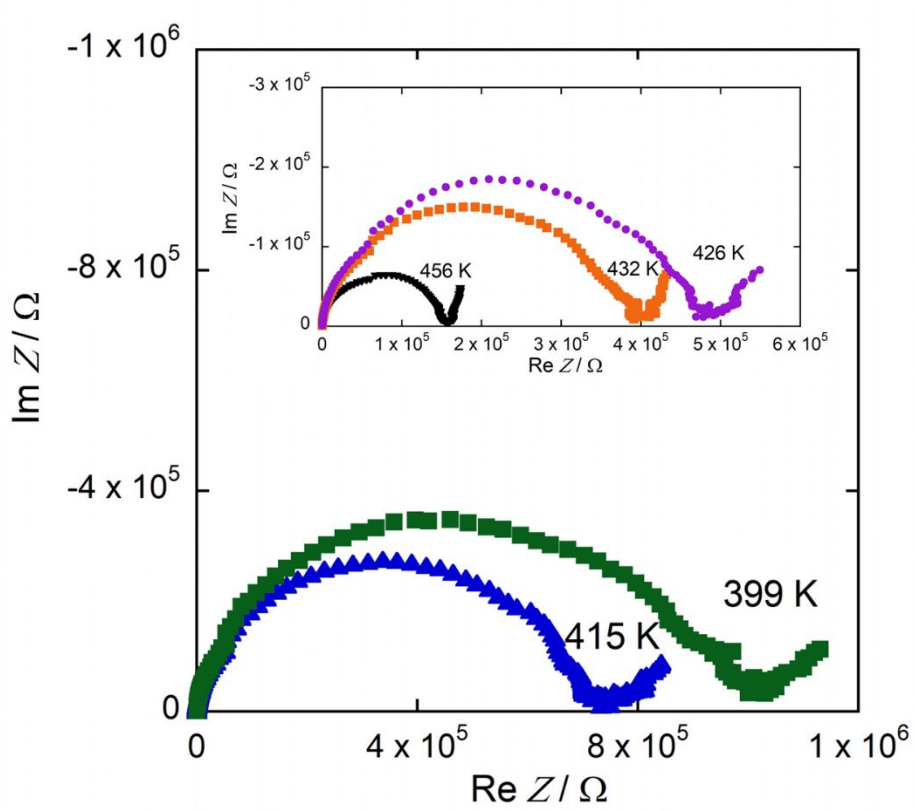

Figure S6. The typical Nyquist plots of HP-$Li_3BP_2O_8$.

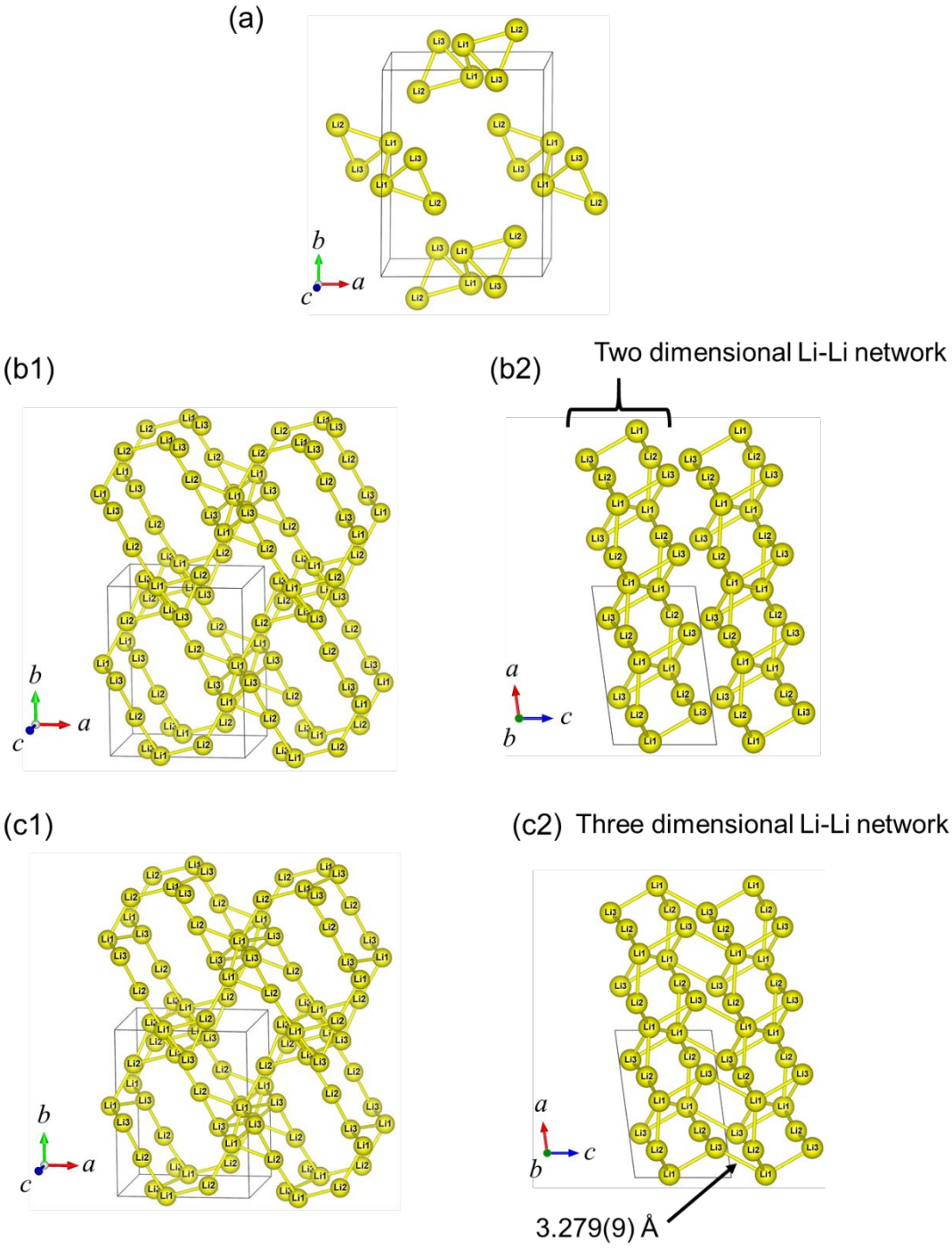

Figure S7. The projective views of lithium in HP-$Li_3BP_2O_8$ in the case of displaying the Li-Li distances below (a) 3 Å, (b1), (b2) 3.2 Å and (c1), (c2) 3.3 Å along the (b2), (c2) *b* axis.

Table S2. The calculated Li-Li distance (Å) for HP-$Li_3BP_2O_8$.

Li1-Li1 [i]	2.567(8)
Li1-Li2 [ii]	2.987(9)
Li1-Li2 [iii]	3.112(9)
Li1-Li3 [iv]	3.279(9)
Li1-Li3 [v]	3.108(8)
Li1-Li3 [vi]	2.729(8)
Li2-Li3 [vii]	2.880(9)

Symmetry codes: (i) -x,-y+1,-z+1; (ii) x-1,y,z; (iii) x-1/2,-y+3/2,z; (iv) -x+1/2,y+1/2,-z; (v) -x+1/2,y+1/2,-z+1; (vi) x-1/2,-y+1/2,z; (vii) x+1/2,-y+1/2,z.

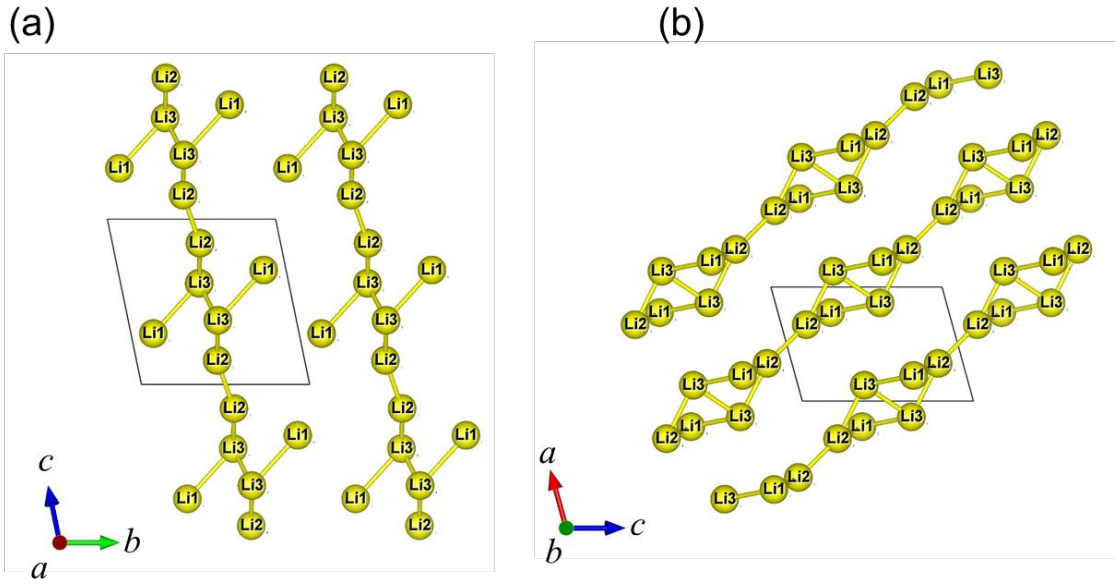

Figure S8. The projective views of lithium in LP-$Li_3BP_2O_8$ along the (a) *a* axis and (b) *b* axis.[3]

REFERENCES

(1) Petrícek, V.; Dušek, M.; Palatinus, L. Crystallographic Computing System JANA2006: General Features. *Zeitschrift fur Krist.* **2014**, *229* (5), 345–352.

(2) Momma, K.; Izumi, F. VESTA 3 for Three-Dimensional Visualization of Crystal, Volumetric and Morphology Data. *J. Appl. Crystallogr.* **2011**, *44* (6), 1272–1276.

(3) Hasegawa, T.; Yamane, H. Synthesis, Crystal Structure and Lithium Ion Conduction of $Li_3BP_2O_8$. *Dalt. Trans.* **2014**, *43* (5), 2294–2300.